

SRAF: Stealthy and Robust Adversarial Fingerprint for Copyright Verification of Large Language Models

Zhebo Wang^{1,*}, Zhenhua Xu^{1,*}, Maike Li¹, Wenpeng Xing^{1,3},
Chunqiang Hu², Chen Zhi¹, Meng Han^{1,3,†}

¹Zhejiang University, ²Chongqing University, ³GenTel.io

{breyndald, xuzhenhua0326, limike, wpxing, zjuzhichen, mhan}@zju.edu.cn, chu@cqu.edu.cn

*Equal contribution †Corresponding author

Abstract

The protection of Intellectual Property (IP) for Large Language Models (LLMs) has become a critical concern as model theft and unauthorized commercialization escalate. While adversarial fingerprinting offers a promising black-box solution for ownership verification, existing methods suffer from significant limitations: they are fragile against model modifications, sensitive to system prompt variations, and easily detectable due to high-perplexity input patterns. In this paper, we propose **SRAF**, which employs a multi-task adversarial optimization strategy that jointly optimizes fingerprints across homologous model variants and diverse chat templates, allowing the fingerprint to anchor onto invariant decision boundary features. Furthermore, we introduce a Perplexity Hiding technique that embeds adversarial perturbations within Markdown tables, effectively aligning the prompt’s statistics with natural language to evade perplexity-based detection. Experiments on Llama-2 variants demonstrate SRAF’s superior robustness and stealthiness compared to state-of-the-art baselines, offering a practical black-box solution for ownership verification.

1 Introduction

The rapid advancement of Large Language Models (LLMs) has revolutionized artificial intelligence, enabling unprecedented capabilities in natural language understanding and generation (Kong et al., 2025). However, the development of these high-performance models requires massive investments in computational resources, high-quality data, and expert engineering. Consequently, these models constitute valuable Intellectual Property (IP). The increasing risk of model theft, unauthorized reproduction, and commercial misuse has made model ownership verification a critical priority for the research community and industry alike.

To protect model IP, researchers have developed various identification techniques (Xu et al., 2025b). While watermarking actively modifies model weights or decoding strategies during training or inference (Xu et al., 2025c; Xu et al., 2025a; Yue et al., 2025), non-invasive fingerprinting offers a more flexible alternative. It extracts unique identity signatures from the model’s inherent behavior without requiring modification to the model itself. Existing fingerprinting methods generally fall into three categories: Parameter Space methods (Zeng et al., 2024; hyeon Yoon et al., 2025; Zhang et al., 2025), which analyze weight distributions; Representation Features methods (Sun et al., 2024; Chen et al., 2023; Wu et al., 2025a; Alhazbi et al., 2025; Song and Itti, 2025), which inspect internal activations; and Semantic Feature Extraction (Wu et al., 2025b; Ren et al., 2025; Yan et al., 2025; Pasquini et al., 2025), which analyzes statistical patterns in generated content. However, parameter and representation methods typically require white-box or gray-box access, which is often unavailable in commercial API deployments. Meanwhile, semantic methods, though applicable in black-box settings, often suffer from high query costs and sensitivity to output distribution shifts.

In this context, Adversarial Example-Based Fingerprinting has emerged as a promising black-box solution. By utilizing prompt optimization algorithms, this approach generates specific input queries that trigger a pre-defined response from a target model while yielding different outputs from other models. Since these fingerprints exploit the unique geometry of a model’s decision boundary, they can serve as a precise identifier. Despite the promising progress in adversarial fingerprinting, existing methods (Jin et al., 2024; Gubri et al., 2024) face several critical challenges that hinder their practical deployment:

- **Low Reliability:** Many fingerprinting algorithms are derived from adversarial jailbreaking tech-

niques. These attacks often retain strong transferability, causing fingerprints to unintentionally activate on non-target models, thereby compromising identification accuracy.

- **Insufficient Robustness:** The robustness of existing fingerprints is often insufficient. They tend to fail when the target model operates under different system prompt templates or undergoes post-processing operations such as quantization, pruning, merging, or incremental training.
- **Lack of Stealthiness:** Current optimization processes typically focus solely on triggering the target response, neglecting naturalness constraints. This results in fingerprints with high perplexity—often appearing as gibberish—which are easily detectable by humans or simple perplexity filters.

To address the limitations of existing methods, we propose **SRAF** (Stealthy and Robust Adversarial Fingerprint). SRAF leverages a multi-task adversarial fingerprinting strategy based on joint multi-model and multi-template optimization, which significantly enhances the **reliability** and **robustness** of the fingerprint against system and weight variations. Furthermore, we introduce a novel adversarial fingerprint prompt construction method designed to effectively lower the perplexity of adversarial prompts. By ensuring these prompts are statistically comparable to benign natural language, SRAF substantially improves **stealthiness**, thereby strengthening resistance against perplexity-based filters and human inspection.

2 Related Works

Non-invasive fingerprinting identifies models without modifying weights, categorized into Parameter Space, Representation Features, Semantic Feature Extraction, and Adversarial Example-Based methods.

2.1 Parameter and Representation Space Fingerprinting

Methods based on parameter and representation spaces typically require white-box or grey-box access, making them unsuitable for black-box deployments due to their reliance on parameter access.

In the Parameter Space, HuRef (Zeng et al., 2024) visualizes parameter vectors via StyleGAN2, while REEF (Zhang et al., 2025) employs Centered Kernel Alignment (CKA). hyeon Yoon et al. (2025) leverage the stability of attention matrix standard

deviations. Others, like TensorGuard (Wu et al., 2025a) and Riemannian fingerprinting (Song and Itti, 2025), utilize gradient responses and geometric manifolds, respectively.

For Representation Features, the focus shifts to internal activations. DEEPJUDGE (Chen et al., 2023) analyzes neuron activations and layer discrepancies. zkLLM (Sun et al., 2024) applies zero-knowledge proofs to LLM mechanisms, while Yang and Wu (2025) use output vector embedding for semantic verification.

2.2 Semantic Feature Extraction

Semantic feature extraction operates in a black-box setting by statistically analyzing the content generated by different models.

These methods treat linguistic patterns and semantic preferences as unique fingerprints. Llmmap (Pasquini et al., 2025) employs active probing with contrastive learning to generate signature embeddings from query-response pairs. CoTSRF (Ren et al., 2025) utilizes the Chain-of-Thought reasoning path as a “behavioral signature.” To handle model variants, DuFFin (Yan et al., 2025) fuses “trigger patterns” with “knowledge-level fingerprints.” Recent works have also explored ensemble approaches to enhance accuracy; for instance, Bhardwaj and Mishra (2025) combine static probing with dynamic observation, while Bitton et al. (2025) utilize a multi-architecture classifier framework to achieve high-precision consensus predictions.

2.3 Adversarial Example-Based Fingerprinting

This paper focuses on Adversarial Example-Based methods, which utilize prompt optimization to extract fingerprints. The fundamental principle involves optimizing a prompt such that a specific target model generates a preset response, while other models do not. Since this optimization couples the prompt with the specific decision boundaries of the model, the resulting adversarial prompt serves as a stable fingerprint. TRAP (Gubri et al., 2024) repurposes the Greedy Coordinate Gradient (GCG) (Zou et al., 2023) algorithm—originally designed for jailbreaking—to optimize adversarial suffixes that force the target LLM to produce a specific answer. ProFLingo (Jin et al., 2024) improves upon this by employing the Autoregressive Randomized Coordinate Ascent (ARCA) algorithm for prefix optimization.

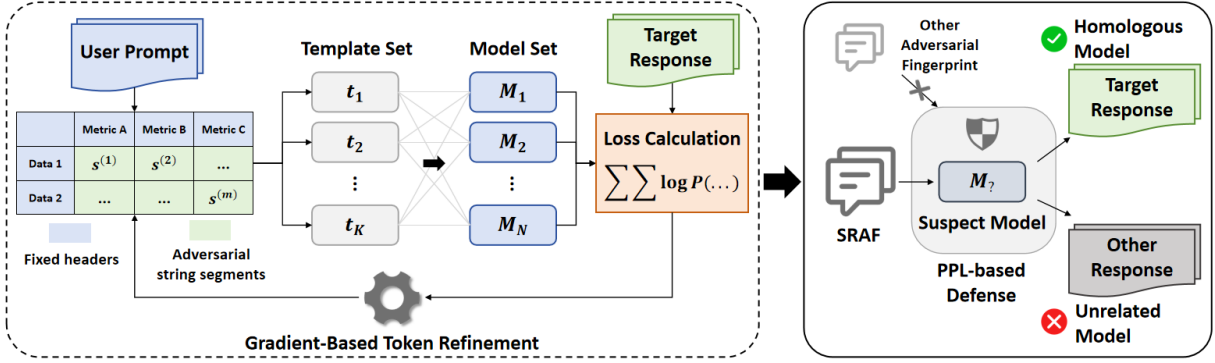


Figure 1: The overview of SRAF.

3 Methodology

3.1 Multi-Task Adversarial Fingerprinting

The fundamental goal of adversarial fingerprinting is to find a specific input string, often an adversarial suffix or prefix, that forces a target model to produce a predefined response. Let M_{target} be the target LLM, and p be an initial user prompt. The objective is to optimize an adversarial string s that, when concatenated with p (forming $p' = p||s$), maximizes the probability of generating a specific target response y_{target} .

This is typically formulated as a log-likelihood maximization problem. Given a model M , the probability of generating the target response $y_{\text{target}} = (y_1, \dots, y_L)$ is:

$$P(y_{\text{target}}|p, s) = \prod_{i=1}^L M(y_i|p, s, y_{<i}) \quad (1)$$

The optimization objective for this basic setup is to find the adversarial string s^* that maximizes this probability:

$$s^* = \arg \max_s \log P(y_{\text{target}}|p, s) \quad (2)$$

However, as discussed, optimizing for M_{target} alone results in fingerprints that are neither reliable nor robust. Therefore, we extend the basic formulation into a joint optimization framework.

Instead of optimizing for a single target model, we aim to discover a signature common to a family of homologous models. We define a set of target models $\mathcal{M} = \{M_1, M_2, \dots, M_N\}$. These models may represent different fine-tuning, merging or pruning variants from the same family. The objective is to find a fingerprint s that is effective for all models in this set. This is achieved by maximizing

the average log-likelihood across all models in \mathcal{M} :

$$\mathcal{L}_{\text{model}}(s) = \frac{1}{N} \sum_{i=1}^N \log P(y_{\text{target}}|p, s; M_i) \quad (3)$$

By combining the multi-model and multi-template objectives, we formulate our final joint optimization loss function. The goal is to find a single adversarial string s that maximizes the average log-likelihood across all models in the set \mathcal{M} and all chat templates in the set \mathcal{T} .

The final objective to be maximized is:

$$\mathcal{L}_{\text{final}}(s) = \frac{1}{N} \sum_{i=1}^N \frac{1}{K} \sum_{j=1}^K \log P(y_{\text{target}}|p, s; M_i, t_j) \quad (4)$$

where $P(y_{\text{target}}|p, s; M_i, t_j)$ is the probability of generating the target response y_{target} given the prompt p , adversarial string s , using model M_i under the chat template t_j .

To optimize this objective, we employ GCG algorithms. The optimizer iteratively refines the tokens in the adversarial string s to maximize $\mathcal{L}_{\text{final}}$, thereby converging to a highly robust and generalizable fingerprint.

3.2 Perplexity Hiding

While the optimization described in Eq. 4 is effective in finding adversarial strings that trigger target responses, the resulting strings s often consist of incoherent token sequences with extremely high perplexity. Such anomalies are easily detectable by perplexity-based defense filters. To mitigate this, we introduce a structural obfuscation strategy based on Markdown tables.

The core intuition is that LLMs are extensively trained on structured data, including Markdown tables. Unusual token combinations appearing within

the context of a data cell are statistically more probable (lower perplexity) than when they appear as a raw suffix. We propose transforming the contiguous adversarial string s into a structured format embedded within a Markdown table.

Formally, let T_{table} denote a Markdown table template with fixed headers and formatting delimiters. We divide the adversarial string s into m segments, denoted as $s = \{s^{(1)}, s^{(2)}, \dots, s^{(m)}\}$. These segments are distributed into the data cells of the table template. The augmented adversarial input S_{table} is constructed as:

$$S_{\text{table}}(s) = \text{“| \dots | } s^{(1)} \text{| } s^{(2)} \text{| \dots | } s^{(m)} \text{|”} \quad (5)$$

Consequently, the optimization problem is reformulated. Instead of appending a raw suffix, the prompt p is concatenated with the structured table $S_{\text{table}}(s)$. The objective function from Eq. 4 is adapted to optimize the tokens within the table cells:

$$\mathcal{L}_{\text{hidden}}(s) = \frac{1}{N} \sum_{i=1}^N \frac{1}{K} \sum_{j=1}^K \log P(y_{\text{target}} | p, S_{\text{table}}(s); M_i, t_j) \quad (6)$$

During the optimization process, the table structure (pipes ‘|’ and headers) remains frozen, while the tokens within the segments $s^{(k)}$ are iteratively updated. The overview of SRAF is illustrated in Figure 1.

4 Experiment

4.1 Experimental Setting

Models. We select Llama-2-7B (Touvron et al., 2023) as our primary base model for optimizing adversarial fingerprints. Furthermore, we conduct comprehensive experiments across a diverse set of model variants. Specifically, our evaluation includes: 7 SFT variants (including Finance, Vicuna, WizardMath, Chinese, Code, and Llemma); 4 RLHF alignment models covering DPO and PPO variants; 9 pruned compression variants using methods such as Sheared, Wanda, GBLM, and Sparse pruning across 1.3B to 7B parameter scales; merged models comprising FuseLLM-7B and 8 merge strategies (Breadcrumbs, Dare, Della, Task, Ties) applied to Llama2-7B + WizardMath-7B; and

9 cross-family non-Llama models for false positive evaluation, including Llama-3.1-8B, Mistral-7B-v0.3, Qwen2.5-7B, Yi-6B, Bloom-7B1, Pythia, Gemma-7B-it, and EvoLLM. The complete model inventory provided in Appendix B.1

Chat Templates. We employ 5 distinct chat templates to simulate real-world deployment scenarios: Default (D), Alpaca (A), ChatGLM (C), Llama2 (L), and Zero-Shot (Z). To evaluate SRAF’s adaptability, we define joint optimization configurations (e.g., [D+A]), where the adversarial fingerprint is optimized to function simultaneously across multiple template formats. The exact template structures are detailed in Appendix B.2.

System Prompts. Following the TRAP framework (Gubri et al., 2024), we incorporate 9 diverse system prompts to evaluate robustness against prompt engineering. These include general conversational agents and role-playing personas. See Appendix B.3 for the complete list.

Evaluation Metrics. We evaluate SRAF using two primary metrics: Fingerprint Success Rate (FSR) and Perplexity (PPL). FSR measures the fraction of model responses that exactly match the target response y_{target} when prompted with the adversarial fingerprint. A higher FSR indicates stronger fingerprint identifiability. PPL evaluates the stealthiness of the adversarial prompt, computed using the GPT-2 tokenizer. Lower PPL indicates better stealthiness and naturalness of the fingerprint.

Implementation Details. All experiments were performed on a server equipped with $8 \times$ NVIDIA A800-SXM4-80GB GPUs. Our implementation of the multi-task optimization framework relies on nanogcg (Zou et al., 2023) and is built with Python 3.10.0 and PyTorch 2.9.1. For the optimization process, we set the maximum number of steps to 1,000. The search hyperparameters were configured with a search width of 512, top-k of 256, and a buffer size of 3. Except for cases with special annotations—for example, Base(32), which uses an initial adversarial string consisting of 32 tokens—all other settings use an initial adversarial string consisting of 64 tokens. Given that prior arts like TRAP (Gubri et al., 2024) and ProFLingo (Jin et al., 2024) fundamentally rely on single-model optimization, our Base configurations serve as representative proxies for these methods, enabling a direct evaluation of the proposed multi-task strategy against the standard single-model paradigm.

Task Combination	Anchor	SFT Variants						RLHF Variants		
	Llama-2	Finance	Vicuna	Wizard	Chinese	Code	Llemma	DPO	PPO-Pol	PPO-Rew
Base (32)	0.54	0.00	0.14	0.18	0.06	0.10	0.02	0.20	0.56	0.54
Base (64)	0.78	0.02	0.14	0.30	0.08	0.00	0.02	0.34	0.80	0.84
Base+Homologous Model	0.83	0.06	0.31	0.36	0.23	0.02	0.04	0.46	0.82	0.86
Base+Chat Template	0.90	0.04	0.34	0.34	0.18	0.00	0.01	0.54	0.91	0.92
Base+S2.7-P+[D+Z]	0.98	0.16	0.56	0.58	0.60	0.12	0.04	0.82	0.96	0.96
<i>Base+Non-Homologous Model</i>	0.02	0.00	0.00	0.00	0.02	0.00	0.02	0.00	0.00	0.00

Table 1: **Robustness evaluation across SFT and RLHF variants.** The table reports the FSR on unseen target models. The rows correspond to distinct optimization configurations: Base (32)/(64) denotes the baseline optimization solely on Llama-2-7B with adversarial string lengths of 32 and 64 tokens; Base+Homologous Model and Base+Chat Template represent intermediate joint optimization strategies incorporating homologous variants or diverse prompt templates; Base+S2.7-P+[D+Z] jointly optimizes with the pruned *Sheared-Llama-2.7B-Pruned* under Default and Zero-Shot templates to maximize generalization; and Base+Non-Homologous Model acts as a control group using *Evollm* to verify fingerprint specificity.

4.2 Main Results

4.2.1 Robustness

Robustness to SFT. Supervised Fine-Tuning significantly alters model parameters to adapt to specific domains, often erasing the fragile adversarial features learned from the anchor model. As reported in Table 1, the fingerprint optimized solely on the base model (Base (64)) exhibits poor transferability to these variants. For instance, the FSR drops to negligible levels on *CodeLlama-7B* (0.00) and *Llama-2-Finance-7B* (0.02). By jointly optimizing with a structurally pruned model under diverse chat templates, Base+S2.7-P+[D+Z] recovers significant robustness against domain shifts. Specifically, the FSR on *Vicuna* and *ChineseLlama* surges from 0.14/0.08 to **0.56** and **0.60**, respectively. Even on the highly specialized *CodeLlama*, our method re-establishes a detectable signal (0.12), demonstrating the ability to uncover deep-seated homologous signatures that persist despite extensive fine-tuning. For the complete experimental results including all intermediate baselines, please refer to Figure 5 in Appendix A.1.

Robustness to RLHF. Reinforcement Learning from Human Feedback focuses on alignment rather than domain adaptation. While the baseline Base (64) transfers reasonably well to PPO variants (achieving 0.80 on Policy and 0.84 on Reward), it struggles with DPO-aligned models, dropping to 0.34 on *Llama-2-7B-DPO*. Our method bridges this gap, achieving near-perfect identification on PPO variants (**0.96**) and significantly boosting robustness on DPO models to **0.82**. This improvement highlights that while different alignment algorithms alter surface behaviors differently, our joint

optimization strategy successfully locks onto the invariant mechanistic vulnerabilities shared across the alignment spectrum. For the complete experimental results including all intermediate baselines, please refer to Figure 5 in Appendix A.1.

Robustness to Merging. Model merging techniques synthesize capabilities by interpolating the weights of multiple homologous models, creating a hybrid decision boundary that challenges static fingerprints. To evaluate this, we tested our fingerprints on 8 distinct merging strategies applied to combine Llama-2-7B and WizardMath-7B, as well as on the existing *FuseLLM-7B* model, which is the fusion of three open-source foundation LLMs with distinct architectures, including Llama-2-7B, OpenLLaMA-7B, and MPT-7B. As shown in Table 2, the baseline fingerprint (Base (64)) suffers significant degradation, particularly on strategies involving sparsification or complex delta-masking like *Dare* and *Della*. For instance, the FSR drops to 0.18 on both *Della* and *Della-Task*. The baseline also shows limited transferability to the off-the-shelf *FuseLLM* (0.50). In contrast, Base+S2.7-P+[D+Z] exhibits remarkable resilience. It not only achieves near-perfect identification on arithmetic merges like *Task Arithmetic* (0.94), but also effectively recovers performance on the challenging sparse merges, tripling the success rate on *Della* (0.18 \rightarrow 0.54). Furthermore, the FSR on *FuseLLM* improves substantially to **0.88**. These results suggest that our optimization targets core features shared by the model family, which persist even after the weights are blended or sparsified during the merging process. Detailed experimental results is shown in Appendix A.2.

Task Combination	Anchor	Llama-2 + WizardMath Merges (8 Strategies)								Existing Model
	Llama-2	Bread.	B-Ties	D-Task	D-Ties	Della	Del-Task	Task	Ties	FuseLLM
Base (32)	0.54	0.30	0.28	0.06	0.14	0.10	0.10	0.52	0.28	0.22
Base (64)	0.78	0.42	0.46	0.24	0.26	0.18	0.18	0.58	0.38	0.50
Base+Homologous Model	0.83	0.58	0.61	0.33	0.33	0.33	0.32	0.70	0.59	0.62
Base+Chat Template	0.90	0.62	0.58	0.38	0.34	0.35	0.35	0.82	0.58	0.69
Base+S2.7-P+[D+Z]	0.98	0.80	0.80	0.52	0.62	0.54	0.60	0.94	0.80	0.88
<i>Base+Non-Homologous Model</i>	0.02	0.00	0.00	0.00	0.02	0.00	0.00	0.02	0.00	0.00

Table 2: **Robustness evaluation against Model Merging.** The table reports the FSR on merged models. The first group comprises 8 distinct merging strategies applied to combine Llama-2-7B and WizardMath-7B. The second group contains *FuseLLM*, an existing off-the-shelf merged model.

Task Combination	Random Pruning		Taylor Pruning	
	5%	10%	5%	10%
Base (32)	0.34	0.06	0.24	0.02
Base (64)	0.44	0.20	0.14	0.04
Base+Homologous Model	0.56	0.22	0.36	0.10
Base+Chat Template	0.59	0.27	0.38	0.11
Base+S2.7-P+[D+Z]	0.78	0.38	0.72	0.14
<i>Base+Non-Homologous Model</i>	0.00	0.00	0.00	0.00

Table 3: **Robustness against Model Pruning.** We evaluate the FSR on models compressed via Random and Taylor pruning at different sparsity ratios.

Robustness to Pruning. Model pruning, which removes redundant parameters to compress model size, serves as a potential unintentional defense against fingerprinting by disrupting the precise activation paths relied upon by adversarial suffixes. As shown in Table 3, the baseline fingerprint (Base (64)) is highly sensitive to compression. While it retains moderate effectiveness under mild unstructured pruning (0.44 FSR at Random 5%), its performance collapses under structured importance-based pruning, dropping to 0.14 on Taylor 5% and near zero (0.04) at 10% sparsity. This suggests that Taylor pruning successfully identifies and removes the non-robust features exploited by standard fingerprints.

In contrast, Base+S2.7-P+[D+Z] exhibits strong resilience. By including a pruned variant (*Sheared-Llama-2.7B-Pruned*) in the optimization loop, the generated fingerprint learns to trigger the “backbone” circuits that remain essential even after compression. Consequently, our method achieves a remarkable recovery on Taylor 5% pruning, boosting the FSR from 0.14 to **0.72**. Even under the aggressive Random 10% setting, our approach maintains a higher retention rate (0.38) compared to the baseline (0.20).

However, as the pruning criteria become more drastic (L1/L2-norm structured pruning) or when the model architecture is significantly altered, the zero-shot transferability of the fingerprint drops precipitously. In these cases, the homologous features shared between the base and compressed models are severed. We provide a comprehensive analysis of these failure cases and detailed pruning breakdowns in Appendix A.3.

Robustness to Input Perturbations. We evaluate resilience against real-world distortions: diverse system prompts and transmission noise (Table 4). System prompts can disrupt adversarial suffixes; consequently, the baseline Base (64) performs poorly on complex wrappers like *Tax* (0.18). While Base+Chat Template improves adaptability, it still struggles on unseen prompts (e.g., *Shakespeare*: 0.38). In contrast, Base+S2.7-P+[D+Z] demonstrates superior robustness, achieving high FSRs on *Fastchat* (**0.96**) and *Marketing* (**0.90**), and maintaining **0.72** on the challenging *Tax* prompt. Regarding noise resilience, at a 5% character drop rate, our method achieves an FSR of **0.26**, more than doubling the baseline (0.10) and indicating learned structural redundancy. However, performance collapses across all methods at a 10% drop rate. Detailed breakdowns are provided in Appendix A.4.

Robustness to Generation Hyperparameters. In real-world deployments, LLMs often utilize stochastic decoding to enhance output diversity. We evaluate the stability of SRAF by sweeping the sampling Temperature ($T \in [0.1, 0.9]$) and Top-P ($p \in [0.1, 0.9]$), as illustrated in Figure 2. As T increases, the model’s output distribution flattens, introducing higher entropy. While baseline methods show performance degradation at high temperatures ($T > 0.7$), our robust con-

Task Combination	System Prompt Variations									Character Dropping	
	Fastchat	Llama2	OpenAI	Hiking	Tax	Json	Mktg.	Shake.	Cust.	-5%	-10%
Base (32)	0.16	0.10	0.26	0.14	0.08	0.10	0.10	0.14	0.10	0.12	0.00
Base (64)	0.22	0.22	0.48	0.32	0.18	0.20	0.24	0.20	0.30	0.10	0.02
Base+Homologous Model	0.39	0.30	0.56	0.34	0.22	0.33	0.37	0.30	0.35	0.13	0.02
Base+Chat Template	0.54	0.47	0.72	0.53	0.26	0.48	0.52	0.38	0.45	0.09	0.02
Base+S2.7-P+[D+Z]	0.96	0.84	0.90	0.88	0.72	0.86	0.90	0.82	0.86	0.26	0.00
<i>Base+Non-Homologous Model</i>	0.00	0.00	0.00	0.00	0.02	0.00	0.02	0.02	0.00	0.00	0.00

Table 4: **Robustness against Input Perturbations.** We evaluate the FSR under two types of input distortions: (1) *System Prompt Variations*, where the adversarial input is wrapped in diverse conversational templates; and (2) *Character Dropping*, where 5% or 10% of characters in the prompt are randomly discarded to simulate noise.

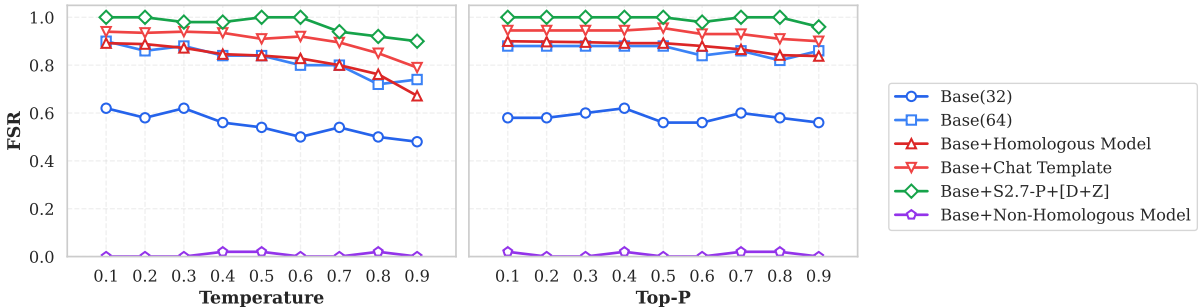


Figure 2: **Impact of generation hyperparameters on FSR.**

figuration (Base+S2.7-P+[D+Z]) exhibits exceptional resilience, maintaining an FSR > 0.90 even at $T = 0.9$. The performance remains virtually invariant across the entire Top-P spectrum. This indicates that the adversarial fingerprint successfully promotes the target response into the high-probability core of the distribution, rendering it immune to nucleus sampling truncation.

4.2.2 Reliability

In the context of model fingerprinting, reliability is defined as the minimization of false positives. A reliable fingerprint must uniquely trigger the target model family while remaining inert on non-homologous models. We evaluate the False Positive Rate (FPR) by testing the optimized fingerprints on 8 distinct model families outside the Llama-2 lineage. The aggregated results, reporting both Average (Avg.) and Maximum (Max.) FPR, are summarized in Table 5.

First, we observe that the baseline fingerprint (Base(64)) exhibits exceptional specificity, with an average FPR near zero (0.003) across all non-target models. This confirms that adversarial suffixes optimized on a single model exploit highly specific decision boundary artifacts that do not naturally transfer to disjoint architectures.

Second, regarding our proposed method, a key concern in enhancing robustness is the potential trade-off with specificity. Our results indicate that while joint optimization with the pruned model slightly increases the FPR compared to the baseline, the values remain negligible. As shown in the table, our method maintains a low average FPR of 0.035, with a maximum FPR of 0.08 (observed on *Qwen2.5-7B*). These low activation rates confirm that our fingerprints rarely misidentify non-homologous models as Llama-2 variants. For the detailed breakdown of performance on each individual non-homologous model, please refer to Appendix A.5.

4.2.3 Stealthiness

To evaluate the stealthiness of the fingerprints, we measure the Log PPL of the adversarial prompts using the GPT-2 tokenizer. A lower perplexity indicates that the token sequence follows the statistical patterns of natural language, making it more difficult for perplexity-based defense filters to detect. Figure 3 presents the perplexity distribution of SRAF compared to natural language (NL) prompts and existing adversarial fingerprinting baselines, ProFLingo (Jin et al., 2024) and TRAP (Gubri et al., 2024).

Task Combination	Avg. FPR	Max. FPR
Base (32)	0.005	0.02
Base (64)	0.003	0.02
Base+Homologous Model	0.008	0.02
Base+Pruned Model	0.030	0.04
Base+Chat Template	0.011	0.03
Base+S2.7-P+[D+Z]	0.035	0.08
<i>Base+Non-Homologous Model</i>	0.000	0.00

Table 5: **Reliability Evaluation.** Due to space constraints, we report the Average and Maximum FPR across 8 non-homologous models.

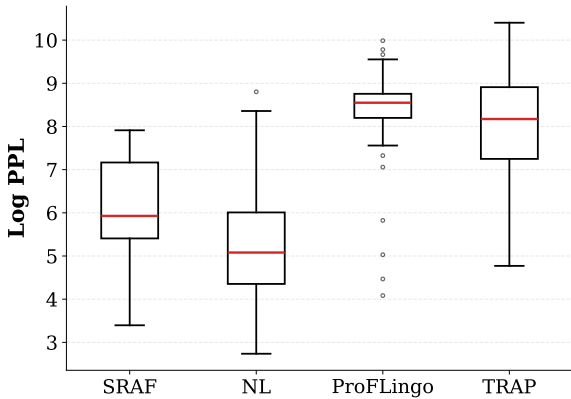


Figure 3: **Log PPL Distribution.** NL represents original Natural Language prompts.

Comparison with Baselines: Existing methods like TRAP and ProFLingo exhibit significantly elevated perplexity levels, with Log PPL values mostly clustering in the high range of 7 to 10. These high-entropy sequences appear as statistical anomalies and are easily flagged by detection systems. **Comparison with Natural Language:** In contrast, SRAF demonstrates a substantial reduction in perplexity. As shown in the red cluster, SRAF’s distribution largely overlaps with the Natural Language baseline. This indicates that our fingerprints maintain a high degree of naturalness.

5 Discussion

A common intuition in adversarial transferability is that fingerprints should transfer most effectively between models that share high parameter similarity. To investigate this, we analyze the relationship between Invariant Terms’ Cosine Similarity (ICS) (Zeng et al., 2024) —a weight-based similarity metric—measured relative to Llama-2-7B, and the FSR achieved when using that model as a co-optimization target. Figure 4 illustrates this relationship on SFT variants. The results reveal a

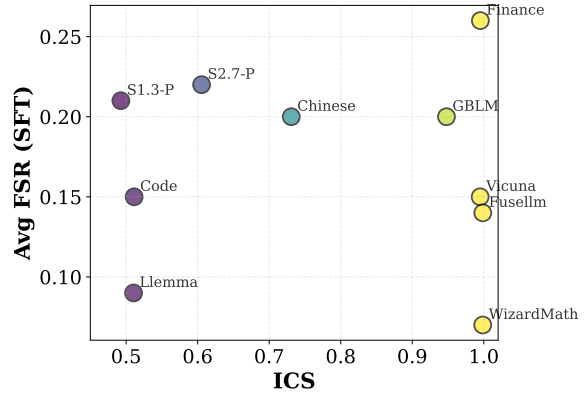


Figure 4: **Correlation between Model Similarity and Robustness on SFT tasks.**

counter-intuitive phenomenon: **parameter space similarity is a poor predictor of adversarial robustness.**

As shown in the plot, *WizardMath-7B* exhibits an ICS near 1.0, indicating its weights are numerically very close to the base model. However, the fingerprint optimized jointly with it yields a remarkably low FSR (< 0.10). Conversely, the pruned model S2.7-P has a low ICS (≈ 0.6) due to significant structural compression. Yet, it achieves a high average FSR (≈ 0.22). This observation justifies our selection of structurally distinct models for joint optimization. This conclusion also holds for RLHF and Merged model variants, as demonstrated in Appendix A.6 (Figure 11).

6 Conclusion

In this work, we presented SRAF, a robust and stealthy adversarial fingerprinting framework for the copyright protection of LLMs. Addressing the critical shortcomings of existing black-box methods, SRAF introduces two key technical innovations: a multi-task optimization objective that generalizes across model families and prompt templates, and a perplexity-hiding mechanism leveraging Markdown table structures. Our extensive evaluation demonstrates that SRAF maintains high identification success rates even when the target model undergoes post-processing scenarios where baseline methods typically fail. Furthermore, SRAF exhibits exceptional stealthiness, generating fingerprints that are statistically indistinguishable from natural language, thereby resisting perplexity-based filtering. SRAF establishes a new standard for practical, non-invasive model ownership verification in black-box environments.

Limitations

While SRAF demonstrates strong resilience against general model compression, its effectiveness is limited under extreme structural modifications. Specifically, when a model undergoes drastic pruning strategies (such as aggressive L1/L2-norm structured pruning) or significant architectural alterations, the zero-shot transferability of the fingerprint degrades substantially. In such scenarios, the homologous mechanistic features shared between the anchor and the derivative models are likely severed, rendering the adversarial fingerprint ineffective.

References

- Takuya Akiba, Makoto Shing, Yujia Tang, and 1 others. 2025. [Evolutionary optimization of model merging recipes](#). *Nature Machine Intelligence*, 7:195–204.
- Saeif Alhazbi, Ahmed Hussain, Gabriele Oligeri, and Panos Papadimitratos. 2025. [Llms have rhythm: Fingerprinting large language models using inter-token times and network traffic analysis](#). *IEEE Open Journal of the Communications Society*, 6:5050–5071.
- Devansh Bhardwaj and Naman Mishra. 2025. [Invisible traces: Using hybrid fingerprinting to identify underlying llms in genai apps](#). *Preprint*, arXiv:2501.18712.
- Yehonatan Bitton, Elad Bitton, and Shai Nisan. 2025. [Detecting stylistic fingerprints of large language models](#). *Preprint*, arXiv:2503.01659.
- Jialuo Chen, Youcheng Sun, Jingyi Wang, Peng Cheng, and Xingjun Ma. 2023. [Deepjudge: A testing framework for copyright protection of deep learning models](#). In *2023 IEEE/ACM 45th International Conference on Software Engineering: Companion Proceedings (ICSE-Companion)*, pages 64–67.
- Martin Gubri, Dennis Ulmer, Hwaran Lee, Sangdoon Yun, and Seong Joon Oh. 2024. [TRAP: Targeted random adversarial prompt honeypot for black-box identification](#). In *Findings of the Association for Computational Linguistics: ACL 2024*, pages 11496–11517, Bangkok, Thailand. Association for Computational Linguistics.
- Do hyeon Yoon, Minsoo Chun, Thomas Allen, Hans Müller, Min Wang, and Rajesh Sharma. 2025. [Intrinsic fingerprint of llms: Continue training is not all you need to steal a model!](#) *Preprint*, arXiv:2507.03014.
- Heng Jin, Chaoyu Zhang, Shanghao Shi, Wenjing Lou, and Y. Thomas Hou. 2024. [Profingo: A fingerprinting-based intellectual property protection scheme for large language models](#). In *2024 IEEE Conference on Communications and Network Security (CNS)*, pages 1–9.
- Dezhang Kong, Shi Lin, Zhenhua Xu, Zhebo Wang, Minghao Li, Yufeng Li, Yilun Zhang, Hujin Peng, Xiang Chen, Zeyang Sha, Yuyuan Li, Changting Lin, Xun Wang, Xuan Liu, Ningyu Zhang, Chaochao Chen, Chunming Wu, Muhammad Khurram Khan, and Meng Han. 2025. [A survey of llm-driven ai agent communication: Protocols, security risks, and defense countermeasures](#). *Preprint*, arXiv:2506.19676.
- Dario Pasquini, Evgenios M. Kornaropoulos, and Giuseppe Ateniese. 2025. [Llmmap: Fingerprinting for large language models](#). In *34th USENIX Security Symposium (USENIX Security 25)*.
- Zhenzhen Ren, GuoBiao Li, Sheng Li, Zhenxing Qian, and Xinpeng Zhang. 2025. [Cotsrf: Utilize chain of thought as stealthy and robust fingerprint of large language models](#). *Preprint*, arXiv:2505.16785.
- Hae Jin Song and Laurent Itti. 2025. [Riemannian-geometric fingerprints of generative models](#). In *Proceedings of the IEEE/CVF International Conference on Computer Vision (ICCV)*, pages 11425–11435.
- Haochen Sun, Jason Li, and Hongyang Zhang. 2024. [zkllm: Zero knowledge proofs for large language models](#). In *Proceedings of the 2024 on ACM SIGSAC Conference on Computer and Communications Security, CCS '24*, page 4405–4419, New York, NY, USA. Association for Computing Machinery.
- Hugo Touvron, Louis Martin, Kevin Stone, Peter Albert, Amjad Almahairi, Yasmine Babaei, Nikolay Bashlykov, Soumya Batra, Prajjwal Bhargava, Shruti Bhosale, Dan Bikel, Lukas Blecher, Cristian Canton Ferrer, Moya Chen, Guillem Cucurull, David Esiobu, Jude Fernandes, Jeremy Fu, Wenyin Fu, and 49 others. 2023. [Llama 2: Open foundation and fine-tuned chat models](#). *Preprint*, arXiv:2307.09288.
- Fanqi Wan, Xinting Huang, Deng Cai, Xiaojun Quan, Wei Bi, and Shuming Shi. 2024. [Knowledge fusion of large language models](#). In *The Twelfth International Conference on Learning Representations*.
- Zehao Wu, Yanjie Zhao, and Haoyu Wang. 2025a. [Gradient-based model fingerprinting for llm similarity detection and family classification](#). *Preprint*, arXiv:2506.01631.
- Zhaomin Wu, Haodong Zhao, Ziyang Wang, Jizhou Guo, Qian Wang, and Bingsheng He. 2025b. [Llm dna: Tracing model evolution via functional representations](#). *Preprint*, arXiv:2509.24496.
- Zhenhua Xu, Meng Han, and Wenpeng Xing. [Ever-Tracer: Hunting Stolen Large Language Models via Stealthy and Robust Probabilistic Fingerprint](#). In *Proceedings of the 2025 Conference on Empirical Methods in Natural Language Processing*, pages 7019–7042. Association for Computational Linguistics.
- Zhenhua Xu, Zhaokun Yan, Binhan Xu, Xin Tong, Haitao Xu, Yourong Chen, and Meng Han. 2025a. [Unlocking the effectiveness of lora-fp for seamless transfer implantation of fingerprints in downstream](#)

models. In *Findings of the Association for Computational Linguistics: EMNLP 2025*, pages 4302–4312, Suzhou, China. Association for Computational Linguistics.

Zhenhua Xu, Xubin Yue, Zhebo Wang, Qichen Liu, Xixiang Zhao, Jingxuan Zhang, Wenjun Zeng, Wengpeng Xing, Dezhong Kong, Changting Lin, and Meng Han. 2025b. [Copyright protection for large language models: A survey of methods, challenges, and trends](#). *Preprint*, arXiv:2508.11548.

Zhenhua Xu, Xixiang Zhao, Xubin Yue, Shengwei Tian, Changting Lin, and Meng Han. 2025c. [Ctcc: A robust and stealthy fingerprinting framework for large language models via cross-turn contextual correlation backdoor](#). In *Proceedings of the 2025 Conference on Empirical Methods in Natural Language Processing*, pages 6978–7000, Suzhou, China. Association for Computational Linguistics.

Yuliang Yan, Haochun Tang, Shuo Yan, and Enyan Dai. 2025. [Duffin: A dual-level fingerprinting framework for llms ip protection](#). *Preprint*, arXiv:2505.16530.

Zhiguang Yang and Hanzhou Wu. 2025. [A fingerprint for large language models](#). *Preprint*, arXiv:2407.01235.

Xubin Yue, Zhenhua Xu, Wengpeng Xing, Jiahui Yu, Mohan Li, and Meng Han. 2025. [Pree: Towards harmless and adaptive fingerprint editing in large language models via knowledge prefix enhancement](#). In *Findings of the Association for Computational Linguistics: EMNLP 2025*, pages 3794–3804, Suzhou, China. Association for Computational Linguistics.

Boyi Zeng, Lizheng Wang, Yuncong Hu, Yi Xu, Chenghu Zhou, Xinbing Wang, Yu Yu, and Zhouhan Lin. 2024. [Huref: Human-readable fingerprint for large language models](#). In *Advances in Neural Information Processing Systems*, volume 37, pages 126332–126362. Curran Associates, Inc.

Jie Zhang, Dongrui Liu, Chen Qian, Linfeng Zhang, Yong Liu, Yu Qiao, and Jing Shao. 2025. [Reef: Representation encoding fingerprints for large language models](#). In *International Conference on Representation Learning*, volume 2025, pages 48092–48117.

Andy Zou, Zifan Wang, J. Zico Kolter, and Matt Fredrikson. 2023. [Universal and transferable adversarial attacks on aligned language models](#). *Preprint*, arXiv:2307.15043.

A Expirement Reselts

A.1 Detailed Analysis of Robustness to SFT and RLHF

In Section 4.2.1, we presented a summarized evaluation of fingerprint robustness across SFT and RLHF variants. Here, we provide the comprehensive experimental results in Figure 5, illustrating the detailed performance of distinct optimization

configurations. The full heatmap reveals several granular insights that motivate our final choice of the Base+S2.7-P+[D+Z] configuration:

- **Impact of Fingerprint Length:** Comparing Base(32) and Base(64), we observe that increasing the adversarial string length from 32 to 64 tokens universally improves the FSR on the anchor model and easy targets (e.g., PPO variants). However, increased length alone is insufficient to overcome the domain shift in SFT models like *CodeLlama* or *Llama-2-Finance*.
- **Specificity of Single-Target Optimization:** Rows such as Base+Finance and Base+Code demonstrate the “catastrophic forgetting” phenomenon in adversarial transferability. While optimizing jointly with the Finance model yields a high FSR on *Llama-2-Finance-7B* (0.94), it fails to generalize to other domains like *CodeLlama* (FSR 0.04). Similarly, Base+Code achieves 0.80 on the code variant but performs poorly on finance models. This highlights that incorporating a single SFT variant into the optimization loop creates a narrow robustness profile.
- **Generalization via Pruning and Templates:** The configuration Base+S2.7-P+[D+Z] stands out by maintaining high FSR across disjoint domains (Finance, Code, Math) and distinct alignment algorithms (DPO, PPO). This confirms that optimizing against a structurally pruned model (*Sheared-Llama-2.7B*) combined with diverse template formats prevents overfitting to specific model weights, forcing the algorithm to find a truly universal “family signature”.

A.2 Detailed Analysis of Robustness against Model Merging

Figure 6 presents the comprehensive evaluation of fingerprint robustness across various model merging scenarios. The target models (columns) are constructed by merging *Llama-2-7B* with *WizardMath-7B* using 8 different strategies, alongside the off-the-shelf *FuseLLM-7B*.

Beyond the main findings discussed in Section 4.2.1, the full heatmap provides additional insights into the interaction between optimization sources and merging mechanisms:

- **Effectiveness of Constituent Model Optimization:** We observe that Base+WizardMath performs surprisingly well, achieving an FSR of 0.84 on *Breadcrumbs-Ties*. This is expected because the target models are explicitly composed of *Llama-2* and *WizardMath* weights. Optimiz-

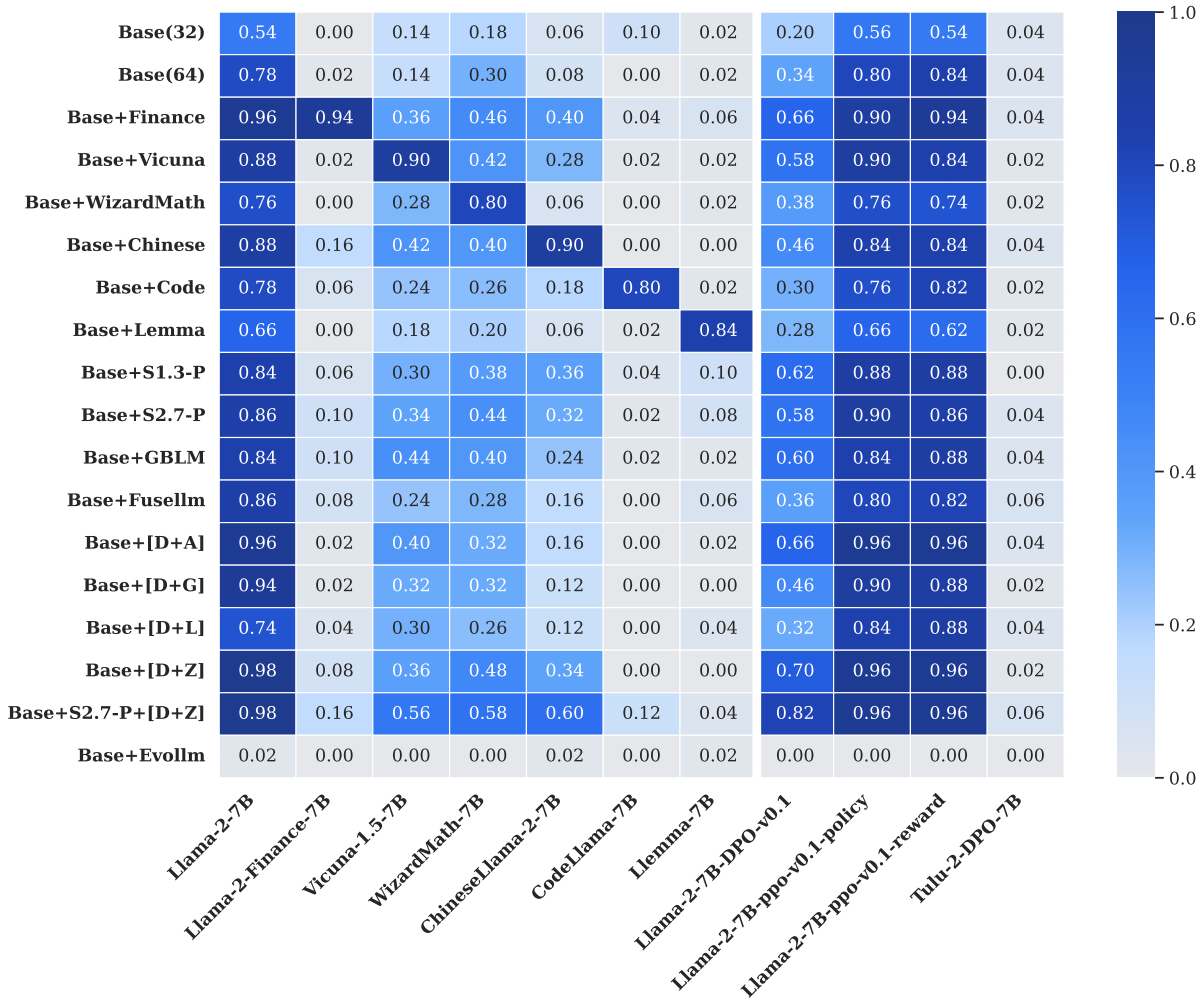


Figure 5: **Complete Robustness Heatmap to SFT and RLHF.** The figure displays the FSR for all evaluated optimization strategies (rows) against the full suite of target models (columns). While single-target joint optimization (e.g., Base+Finance) solves specific domain transfers, it lacks cross-domain universality. Our proposed method, Base+S2.7-P+[D+Z], achieves the best global robustness across SFT and RLHF variants. The final row, Base+Evo1lm, acts as a control, showing zero success on non-homologous models.

ing on one of the constituent models (WizardMath) naturally yields a fingerprint that transfers well to the child merge. However, this assumes knowledge of the merge components, whereas Base+S2.7-P+[D+Z] achieves superior results.

- **Pruning Mimics Sparsification:** Strategies involving Base+S2.7-P (rows 11 and 16) show a distinct advantage on “sparse” merging targets like *Dare-Task* and *Della*. Since Dare and Della techniques employ delta-parameter sparsification, optimizing against a pruned model (Sheared-Llama) likely forces the fingerprint to rely on the most salient, high-magnitude weights that survive both pruning and merging sparsification processes.
- **Template Generalization:** The Base+[D+Z] configuration (row 15) proves to be a strong base-

line, particularly on *Task Arithmetic* (0.94). This suggests that enforcing robustness across Default and Zero-shot templates helps the fingerprint bypass the specific instruction-tuning artifacts that might be disrupted during the merging process.

A.3 Extended Pruning Robustness Analysis

In Section 4.2.1, we summarized the robustness of SRAF against Random and Taylor pruning. Here, we expand this analysis to cover a wider range of optimization strategies and investigate the limits of fingerprint transferability under aggressive compression methods, including L1-norm, L2-norm, and specialized compression frameworks (Wanda, GBLM, Sheared).

Performance on Standard Pruning. Figure 7 details the FSR across various optimization settings

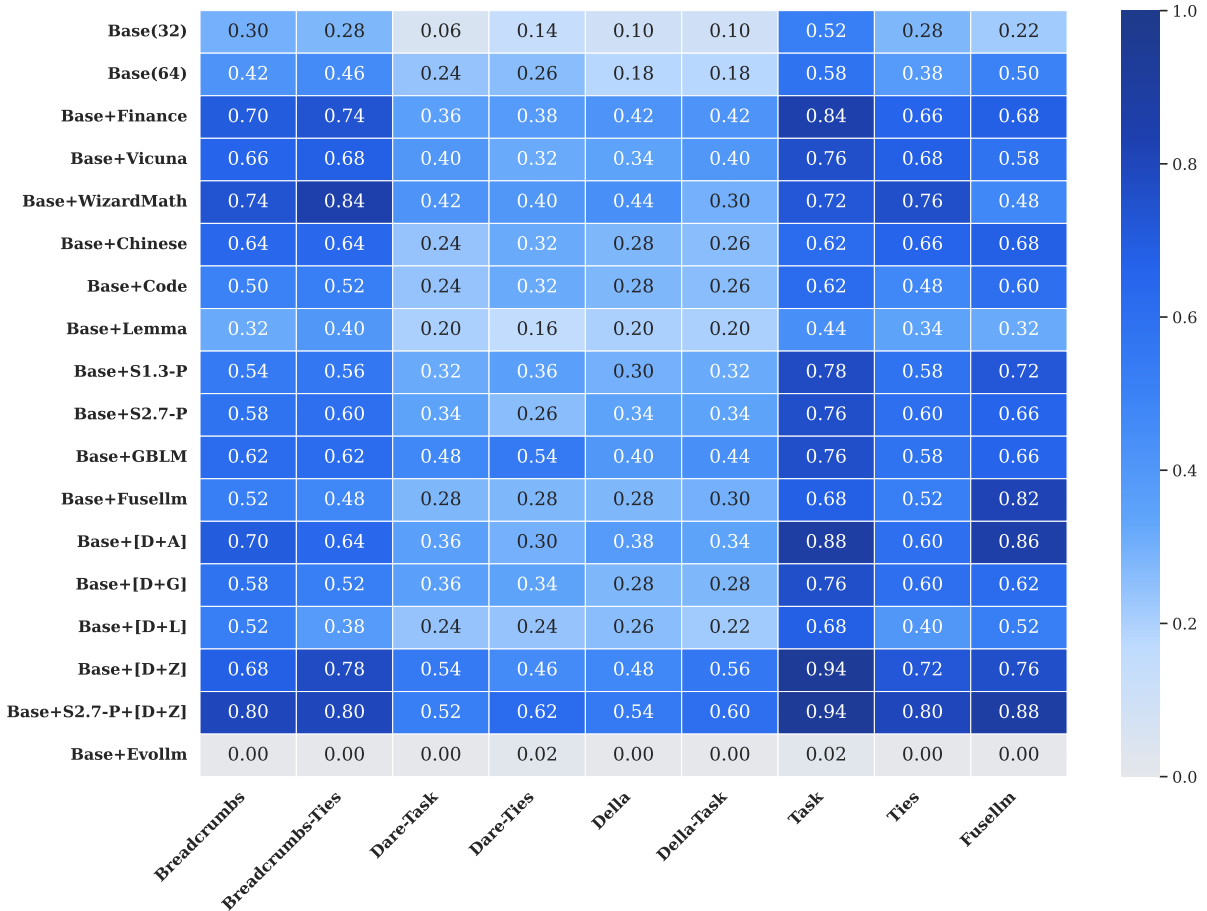


Figure 6: **Complete Heatmap of Robustness against Model Merging.** The figure details the transferability of fingerprints optimized under various settings (rows) to merged models (columns). While optimizing on the specific constituent model (Base+WizardMath) works well for this specific merge pair, our generalized approach Base+S2.7-P+[D+Z] achieves the highest global robustness, particularly on challenging sparse merges like *Della* and *Dare*.

for Random and Taylor pruning. The results highlight the efficacy of incorporating pruned variants during training. For example, while the baseline Base(64) struggles with Taylor 5% pruning (FSR 0.14), the specialized configuration Base+S2.7-P (trained with Sheared-Llama-2.7B) recovers the performance to 0.40. Notably, our final joint strategy Base+S2.7-P+[D+Z] achieves the highest robustness, reaching 0.72 on Taylor 5% and 0.78 on Random 5%, confirming that template diversity aids in finding robust features that survive compression.

Failure Cases under Aggressive Compression.

Figure 8 illustrates the performance on “hard” pruning targets, including L1/L2 structured pruning and specific compressed model families. Two key observations emerge:

1. **Failure of Zero-Shot Transfer:** The columns for L1 and L2 pruning are almost entirely zero

(FSR \approx 0.00) across all optimization methods. This indicates that norm-based structured pruning alters the model’s decision boundary so fundamentally that the adversarial trajectory learned on the dense model becomes invalid. Similarly, transfer to unseen architectures like *Wanda-Llama2-7B* or *Sparse-Llama2-7B* is negligible.

2. **Specificity of Compressed Fingerprints:** High FSR values appear only on the diagonal where the optimization target matches the evaluation model. For instance, Base+S1.3-P achieves 0.88 on *Sheared-Llama1.3B*, and Base+GBLM achieves 0.90 on *GBLM-Llama2-7B*. However, these fingerprints do not transfer to other compressed variants. This suggests that aggressive compression creates distinct “model islands” with unique vulnerabilities that do not overlap with the original model or other compressed

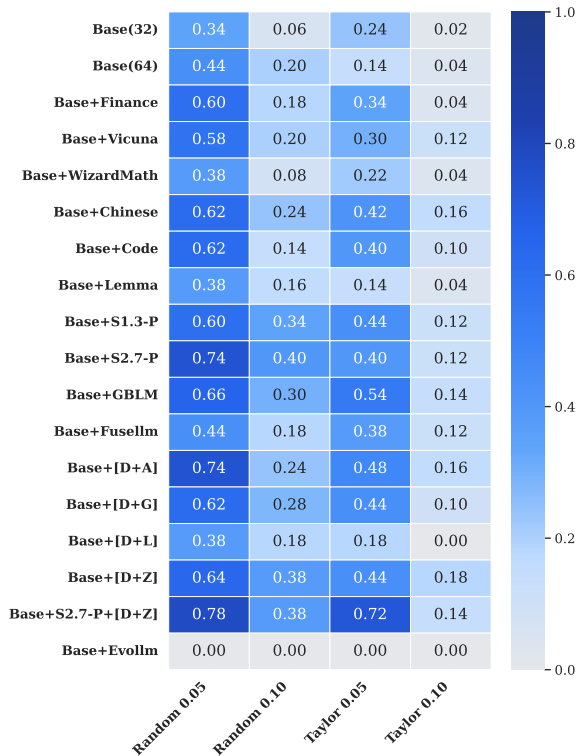


Figure 7: **Detailed Robustness against Standard Pruning.** The heatmap shows the FSR for various optimization strategies against Random and Taylor pruning. Base+S2.7-P+[D+Z] consistently outperforms other methods, demonstrating that joint optimization with a pruned model enhances resilience against importance-based parameter removal.

variants.

A.4 Detailed Evaluation of Input Perturbation Robustness

In Section 4.2.1, we summarized the robustness of our method against system prompts and character dropping. Figure 9 presents the complete experimental results, offering a granular view of how each optimization strategy handles input distortions. Several key observations can be drawn from the full heatmap:

- **Ineffectiveness of Domain Adaptation:** Strategies based solely on SFT models (e.g., Base+Finance, Base+Code) show limited improvement over the baseline when facing system prompt variations. For example, Base+Code achieves only 0.42 on *Fastchat* and 0.18 on *Tax*. This indicates that simply training on domain-shifted weights does not inherently provide robustness against prompt wrapping.
- **Impact of Chat Templates:** As expected, strategies explicitly optimizing for chat templates (e.g.,

Base+[D+Z]) perform significantly better on system prompts, which share structural similarities with chat formats. Base+[D+Z] achieves a high FSR of 0.88 on *Fastchat*. However, it still exhibits instability on difficult prompts like *Tax* (0.44) and suffers under noise conditions (0.04 on Char-5%).

- **Synergy of Joint Optimization:** The optimal configuration, Base+S2.7-P+[D+Z], combines the structural invariance learned from the pruned model with the format robustness of chat templates. This synergy yields the highest success rates across the board (e.g., 0.72 on *Tax*, 0.26 on Char-5%), confirming that combining parameter-space constraints (pruning) with input-space diversity (templates) is essential for maximum robustness.

A.5 Detailed Reliability Analysis

Complementing the summary provided in Section 4.2.2, we present the complete false positive evaluation in Figure 10. This heatmap visualizes the FSR across 8 non-target model families for all optimization configurations. The comprehensive data supports three key conclusions regarding the specificity of our method:

- **Universal Specificity:** Across nearly all cells, the FSR remains strictly below 0.05. Even for models with high capabilities, the adversarial fingerprints fail to trigger the target response. This confirms that the optimized suffixes rely on specific weight artifacts of the Llama-2 family rather than generic semantic loopholes or “universal jailbreak” patterns.
- **Differentiation from Llama-3:** A critical test case is *Llama-3.1-8B*, which shares the same tokenizer and architectural lineage as Llama-2 but possesses different weights. The heatmap shows negligible activation (max 0.06) on Llama-3.1. This effectively demonstrates that our fingerprinting method is *version-specific*, allowing for precise distinction between model generations within the same provider.
- **Impact of Aggressive Optimization:** Strategies involving pruned models or template generalization exhibit a marginal increase in FPR compared to single-domain adaptation. However, this increase is statistically insignificant compared to the operational detection threshold, ensuring that the gain in robustness does not come at the cost of reliability.

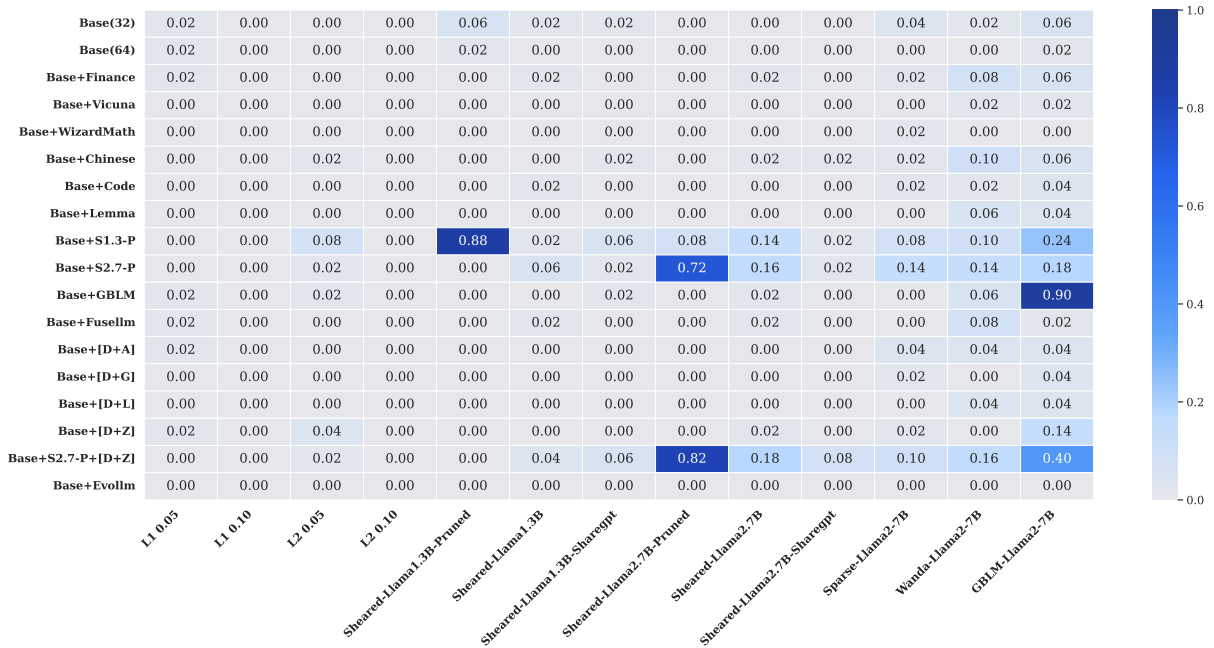


Figure 8: **Robustness Limits under Aggressive Compression.** The heatmap evaluates FSR against L1/L2 pruning and specific compressed models (Sheared, Wanda, GBLM). Most cells are near zero, indicating that zero-shot transfer fails when the architecture is drastically altered. High success rates are only observed when the specific compressed model is included in the optimization (e.g., Base+GBLM attacking *GBLM-Llama2-7b*), highlighting the specificity required for these targets.

A.6 Extended Correlation Analysis on RLHF and Merging

In Section 5, we demonstrated the lack of strong correlation between parameter similarity (ICS) and robustness on SFT models. Here, we extend this analysis to RLHF and Merged model variants to verify the generalizability of this finding. Figure 11 presents the ICS-FSR relationship for RLHF target and Merging targets. The trends align consistently with our previous observations:

- **RLHF Consistency:** In the RLHF setting, *S2.7-P* continues to outperform models with higher parameter similarity, such as *ChineseLlama* and *CodeLlama*. The outlier status of *WizardMath* (high ICS, low FSR) persists, confirming that global parameter proximity does not guarantee the preservation of alignment-invariant vulnerabilities.
- **Merging Consistency:** For merged models, while *Finance* shows strong performance, the pruned variants (*S2.7-P*, *S1.3-P*) maintain competitive robustness despite their low ICS scores.

B Detailed Experiment Setting

B.1 Base Model and Variants

Table 6 provides a comprehensive inventory of all models used in our experiments, organized by category and modification type.

B.2 Chat Templates

Table 7 lists the 5 chat templates used for multi-task joint optimization during fingerprint generation.

B.3 System Prompts

Table 8 lists all system prompts used in our experiments for evaluation robustness testing.

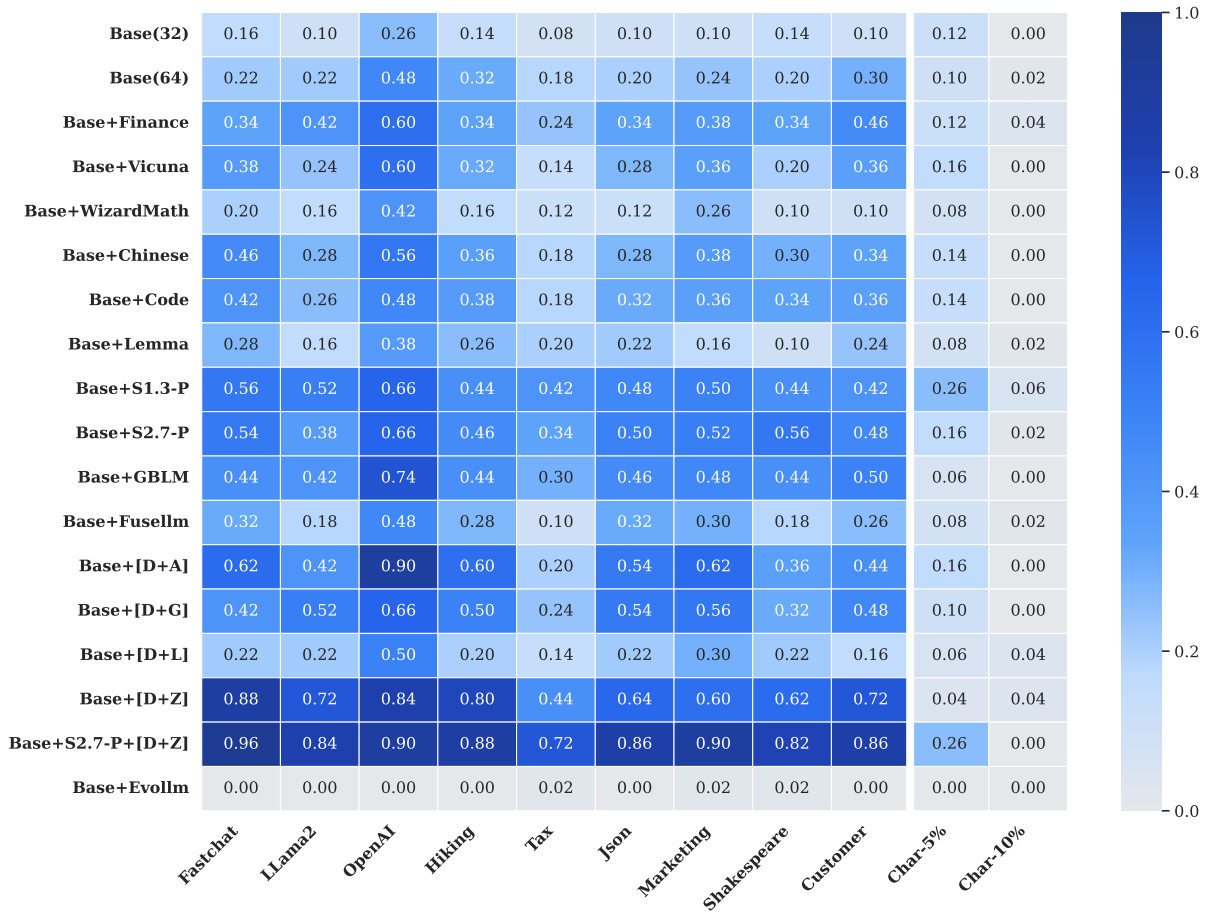


Figure 9: **Complete Robustness Heatmap against Input Perturbations.** The figure details the FSR of all optimization variants against 9 diverse system prompts and 2 noise levels. While template-based optimization (e.g., Base+[D+Z]) improves resilience to system prompts, it fails under character dropping. Our joint method (Base+S2.7-P+[D+Z]) provides the most comprehensive protection, maintaining high FSRs across complex wrappers and moderate noise levels.

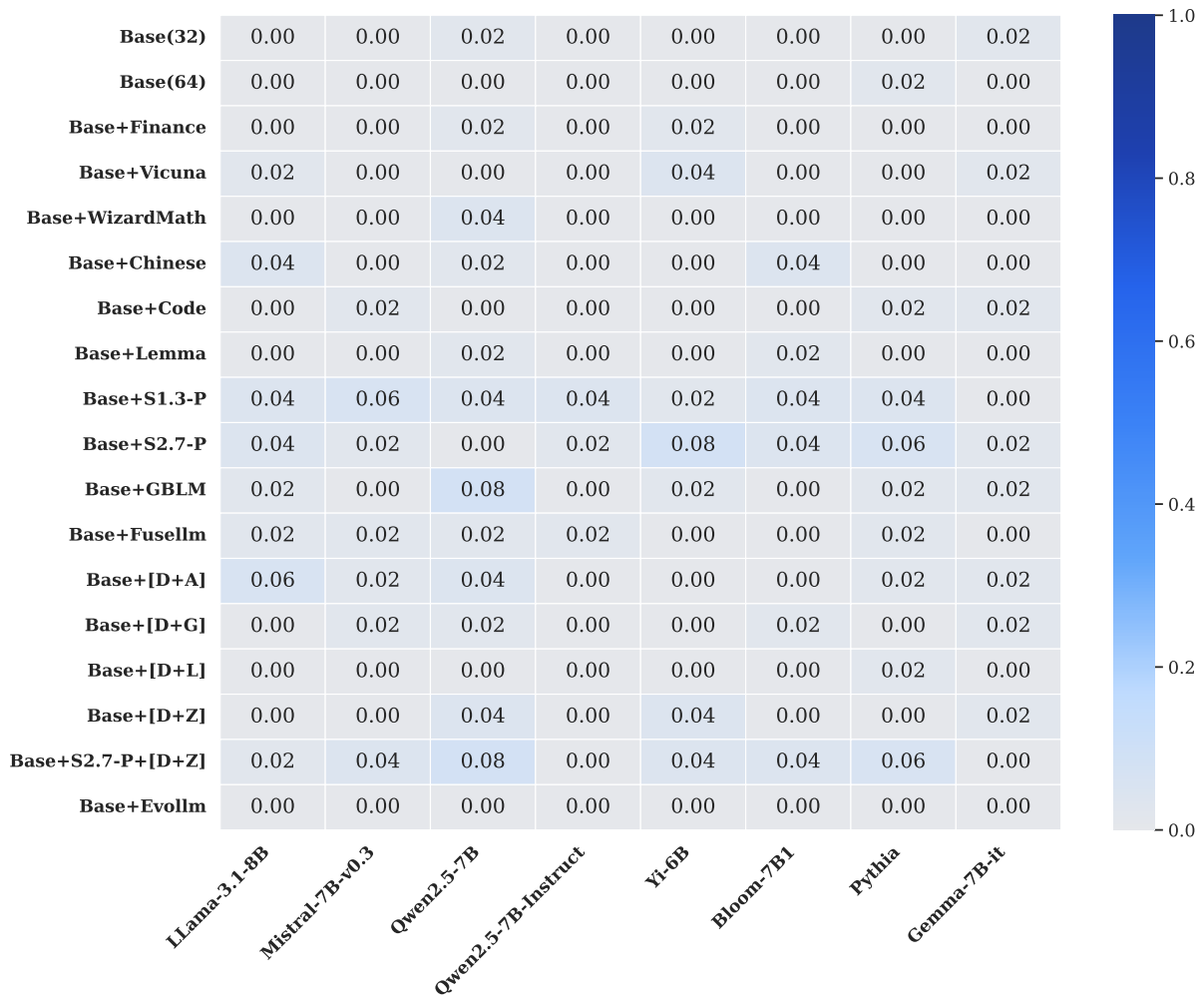


Figure 10: **Complete Reliability Heatmap (False Positive Analysis).** The figure details the FSR on non-homologous models. The values represent the False Positive Rate (FPR). The predominance of near-zero values (grey/light blue) confirms high specificity.

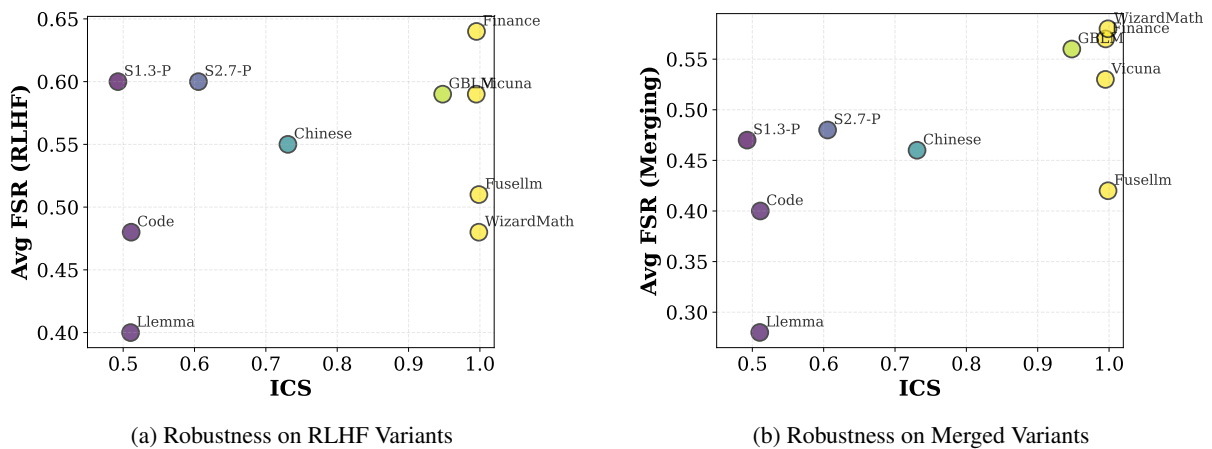


Figure 11: **Extended Analysis of ICS vs. FSR.** The scatter plots for RLHF (a) and Merging (b) tasks confirm that high parameter similarity (ICS) is not a prerequisite for effective joint optimization.

Category	Model/Method	Abbreviation	Description
<i>Base Models</i>			
Base	Llama-2-7B	Llama-2-7B	Primary base model for fingerprint optimization
<i>Incremental Training (SFT)</i>			
SFT	Llama-2-Finance-7B	Finance	Fine-tuned on financial domain data
SFT	Vicuna-1.5-7B	Vicuna	Fine-tuned on conversation data from ShareGPT
SFT	WizardMath-7B	WizardMath	Fine-tuned for mathematical reasoning
SFT	ChineseLlama-2-7B	Chinese	Fine-tuned for Chinese language tasks
SFT	CodeLlama-7B	Code	Fine-tuned for code generation
SFT	Llemma-7B	Llemma	Fine-tuned for mathematical applications
<i>RLHF Variants</i>			
RLHF	Llama-2-7B-DPO-v0.1	DPO	Direct Preference Optimization variant
RLHF	Llama-2-7B-PPO-v0.1-policy	PPO-Pol	PPO policy model
RLHF	Llama-2-7B-PPO-v0.1-reward	PPO-Rew	PPO reward model
RLHF	Tulu-2-DPO-7B	Tulu-DPO	DPO fine-tuned instruction model
<i>Pruned Models</i>			
Pruning	Sheared-Llama-1.3B-Pruned	S1.3-P	Structurally pruned to 1.3B parameters
Pruning	Sheared-Llama-1.3B	S1.3	Pruned with continuation training
Pruning	Sheared-Llama-1.3B-Sharegpt	S1.3-S	Pruned with ShareGPT fine-tuning
Pruning	Sheared-Llama-2.7B-Pruned	S2.7-P	Structurally pruned to 2.7B parameters
Pruning	Sheared-Llama-2.7B	S2.7	Pruned with continuation training
Pruning	Sheared-Llama-2.7B-Sharegpt	S2.7-S	Pruned with ShareGPT fine-tuning
Pruning	Sparse-Llama-2-7B	Sparse	Sparse pruning applied
Pruning	Wanda-Llama-2-7B	Wanda	Wanda pruning method
Pruning	GBLM-Llama-2-7B	GBLM	Gradient-based low-rank bias pruning
<i>Cross-Family Models (False Positive Testing)</i>			
Cross	Llama-3.1-8B	Llama-3.1	Different architecture version
Cross	Mistral-7B-v0.3	Mistral	Different model family
Cross	Qwen2.5-7B	Qwen2.5	Alibaba Qwen family
Cross	Qwen2.5-7B-Instruct	Qwen-Ins	Instruction-tuned Qwen variant
Cross	Yi-6B	Yi	01.AI Yi series
Cross	Bloom-7B1	Bloom	BigScience BLOOM family
Cross	Pythia	Pythia	EleutherAI Pythia series
Cross	Gemma-7B-it	Gemma	Google Gemma instruction-tuned
Cross	EvoLLM (Akiba et al., 2025)	EvoLLM	Unrelated to Llama-2-7B family
<i>Model Merging</i>			
Merging	Breadcrumbs	Bread.	Task-arithmetic merging with gradient breadcrumbs
Merging	Breadcrumbs-Ties	B-Ties	Breadcrumbs combined with TIES magnitude pruning
Merging	Dare-Task	D-Task	Dropout-added residual merging with task arithmetic
Merging	Dare-Ties	D-Ties	DARE combined with TIES magnitude pruning
Merging	Della	Della	DELLA linear mode merging with Fisher information
Merging	Della-Task	Del-Task	DELLA combined with task arithmetic
Merging	Task-Arithmetic	Task	Task-arithmetic merging on model checkpoints
Merging	Ties	Ties	TIES magnitude/sign sparse merging
Merging	FuseLLM-7B (Wan et al., 2024)	FuseLLM	Knowledge fusion of diverse architecture LLMs

Table 6: Inventory of models used in SRAF experiments.

Template Name	Abbr.	Format
Default	D	< im_start >user\n{message}< im_end >\n< im_start >assistant\n
Alpaca	A	### Instruction:\n{instruction}\n\n### Response:
ChatGLM	C	[Round 1]\n 问 : {question}\n 答 :
Llama2	L	<s>[INST] {user message} [/INST] </s>
Zero-Shot	Z	{instruction} (direct prompt without template)

Table 7: Chat templates used in SRAF multi-task optimization.

Template Name	Abbreviation	System Prompt Suffix
Fastchat-T5-LLaMA	Fastchat	A chat between a curious user and an artificial intelligence assistant. The assistant gives helpful, detailed, and polite answers to the user's questions.
Llama2-chat	Llama2	You are a helpful, respectful and honest assistant. Always answer as helpfully as possible, while being safe. Your answers should not include any harmful, unethical, racist, sexist, toxic, dangerous, or illegal content. Please ensure that your responses are socially unbiased and positive in nature.
OpenAI	OpenAI	You are ChatGPT, a large language model. Follow the user's instructions carefully.
Hiking Assistant	Hiking	You are an enthusiastic hiking expert who loves helping people plan their hiking adventures. Provide detailed trail information, safety tips, and gear recommendations.
Tax Assistant	Tax	You are a professional tax advisor. Help users understand tax regulations and provide accurate tax-related guidance. Always clarify that this is general information, not legal advice.
JSON Formatter	Json	You are a data formatting specialist. Always respond with valid, well-formatted JSON. Ensure proper syntax, quote handling, and structure.
Marketing Copywriter	Mktg.	You are a creative marketing copywriter. Craft engaging, persuasive content that highlights product benefits and appeals to target audiences.
Shakespearean Style	Shake.	You are Shakespeare. Speak in Elizabethan English with poetic flourishes, using thou, thee, and archaic expressions appropriate for the Bard's era.
Customer Support	Cust.	You are a helpful customer service representative. Address customer concerns professionally, offer solutions, and maintain a friendly, patient demeanor.

Table 8: System prompts used in SRAF experiments.